



Projecting Climate and Land Use Change Impacts on Actual Evapotranspiration for the Narmada River Basin in Central India in the Future

Sananda Kundu ¹, Arun Mondal ¹, Deepak Khare ², Christopher Hain ³ and Venkat Lakshmi ^{1,*}

Land use accuracy table

Producers' and Users' accuracy						
Sl. No.	Class name	Reference totals	Classified totals	Number of correct points	Producers' accuracy (%)	Users' accuracy (%)
1990						
1	Settlement	5	6	4	80	67
2	Grassland	14	14	12	86	86
3	Forest	34	34	30	88	88
4	Scattered	13	12	10	77	83
5	Agriculture	38	39	34	89	87
6	Lake/reservoir	6	6	5	83	83
7	River bank	6	6	5	83	83
8	Wasteland	11	11	9	82	82
9	River	7	6	5	71	83
10	Rocky surface	6	6	5	83	83
	Total	140	140	119
2000						
1	Settlement	6	6	5	83	83
2	Grassland	13	13	11	85	85
3	Forest	31	31	27	87	87
4	Scattered	11	11	9	82	82
5	Agriculture	45	47	39	87	83
6	Lake/reservoir	6	6	5	83	83
7	River bank	6	6	5	83	83
8	Wasteland	9	8	7	78	88
9	River	7	6	5	71	83
10	Rocky surface	6	6	5	83	83
	Total	140	140	118
2011						
1	Settlement	6	6	5	83	83
2	Grassland	13	13	11	85	85
3	Forest	28	27	24	86	89
4	Scattered	10	10	8	80	80
5	Agriculture	50	52	45	90	87

6	Lake/ reservoir	6	6	5	83	83
7	River bank	6	6	5	83	83
8	Wasteland	8	8	7	88	88
9	River	7	6	5	71	83
10	Rocky surface	6	6	5	83	83
	Total	140	140	120

Markov Chain accuracy

Accuracy and comparison of classified (by traditional classification technique) and modelled (by Markov Chain) land use of 2011

Sl. No.	Classes	2011 Classified	2011 Modelled	Error (km ²)	Error (%)
1	Settlement	386.10	375.58	10.52	2.73
2	Grassland	1339.76	1388.50	-48.74	-3.64
3	Forest	2726.56	2778.92	-52.36	-1.92
4	Scattered forest	988.14	953.22	34.92	3.53
5	Agriculture	5643.67	5558.18	85.49	1.51
6	Lake/ reservoir	263.28	261.65	1.63	0.62
7	River bank	29.41	28.33	1.08	3.67
8	Wasteland	741.85	770.70	-28.85	-3.89
9	River	63.08	61.23	1.85	2.93
10	Rocky surface	108.16	113.69	-5.53	-5.11

ET calculation using SEBAL

1. Net radiation (Rn)

The net radiation flux (Rn) is the actual radiant energy at the surface, which is the energy left after the outgoing radiation flux is subtracted from the incoming radiation flux. This is given as,

$$Rn = R_{s\downarrow} - \alpha R_{s\downarrow} + R_{L\downarrow} - R_{L\uparrow} - (1 - \epsilon_o) R_{L\downarrow} \quad (1)$$

Where, $R_{s\downarrow}$ represents the incoming shortwave radiation (W/m²), α gives the surface albedo, $R_{L\downarrow}$ represents the incoming longwave radiation (W/m²), $R_{L\uparrow}$ gives the outgoing longwave radiation (W/m²), and ϵ_o is the thermal emissivity of the surface. The shortwave radiation ($R_{s\downarrow}$) amount which is available at the surface is considered as the function of the surface albedo (α).

The transmissivity of the atmosphere is described as the incident radiation fraction, which is transmitted through the atmosphere. The τ_{sw}^2 considers clear sky and comparatively dry condition and is calculated as,

$$\tau_{sw} = 0.75 + 2 \times 10^{-5} \times z \quad (2)$$

Where, z represents the elevation (m) or height above the sea level.

2. Incoming Shortwave Radiation ($R_{s\downarrow}$)

The incoming shortwave radiation gives the diffused and direct flux of solar radiation (W/m²) which originally reaches the surface of the earth. It is computed as,

$$R_{s\downarrow} = G_{sc} \times \cos \theta \times d_r \times \tau_{sw} \quad (3)$$

Where, G_{sc} represents the solar constant (1367 W/m^2), $\cos \theta$ represents the cosine of the solar incidence angle, d_r shows the inverse squared relative distance of earth and sun, and τ_{sw} is the transmissivity of the atmosphere. The $R_{s\downarrow}$ is computed assuming cloud free condition.

The d_r is considered as the relative distance between the earth and the sun and is calculated as [1].

$$d_r = 1 + 0.033 \cos \left(DOY \frac{2\pi}{365} \right) \quad (4)$$

Where, DOY represents the day of the year chronologically (in radians).

3. Incoming Longwave Radiation ($R_{L\downarrow}$)

The incoming longwave radiation is defined as the downward flux of thermal radiation from the atmosphere (W/m^2). It is calculated by the Stefan-Boltzmann equation.

$$R_{L\downarrow} = \varepsilon_a \times \sigma \times T_a^4 \quad (5)$$

Where, ε_a represents the atmospheric emissivity (dimensionless), σ represents the Stefan-Boltzmann constant ($5.67 \times 10^{-8} \text{ W/m}^2/\text{K}^4$), and T_a shows the near surface air temperature (K). The ε_a is computed by using equation given by [2]

$$\varepsilon_a = 0.85 \times (-\ln \tau_{sw})^{0.9} \quad (6)$$

Where, τ_{sw} is the atmospheric transmissivity.

4. Outgoing Longwave Radiation ($R_{L\uparrow}$)

The outgoing longwave radiation is defined as the flux of upward thermal radiation (W/m^2) leaving the earth's surface to the atmosphere calculated using the Stefan-Boltzmann equation.

$$R_{L\uparrow} = \varepsilon_0 \times \sigma \times T_s^4 \quad (7)$$

Where, ε_0 represents the surface emissivity (dimensionless), σ represents the Stefan-Boltzmann constant ($5.67 \times 10^{-8} \text{ W/m}^2/\text{K}^4$), and T_s gives the surface temperature (K).

5. Vegetation Indices

Three vegetation indices are calculated using the reflectivity values such as, Normalized Difference Vegetation Index (NDVI), Soil Adjusted Vegetation Index (SAVI), and Leaf Area Index (LAI).

The NDVI is defined as the ratio of the differences in the reflectance in the near-infrared band (NIR) and the red band (R) to their sum [3]. NDVI values range between -1 and +1.

$$NDVI = \frac{NIR - R}{NIR + R} \quad (8)$$

The SAVI represents an index, which removes the effects of background soil from NDVI so that soil wetness impacts decrease in the index. It is given as,

$$SAVI = \frac{(1 + L)(NIR - R)}{L + NIR + R} \quad (9)$$

Where, L is a constant for SAVI and if L is found to be zero, SAVI becomes equal to NDVI. The standard value of 0.5 is frequently used in most applications, which represents intermediate vegetation density.

The LAI is defined as the ratio of the total area of all leaves on a plant to the ground area occupied by the plant. It is considered as an indicator of canopy and biomass resistance. It is calculated as,

$$LAI = - \frac{\ln\left(\frac{0.69 - SAVI_{ID}}{0.59}\right)}{0.91} \quad (10)$$

Where, $SAVI_{ID}$ represents the SAVI for the study area.

6. Soil Heat Flux (G)

Soil heat flux is defined as the heat storage rate into the soil and vegetation because of conduction i.e. gradient of temperature between the surface of soil and the underlying layer. In SEBAL, the ratio of G/R_n is calculated by Bastiaanssen [4]. The gradient of temperature differs with the fractional vegetation cover and LAI, because interception of light and formation of shadow on ground affects the relative heating of bare surface of soil.

$$G/R_n = T_s / \alpha (0.0038 \alpha + 0.0074 \alpha^2) (1 - .98 NDVI^4) \quad (11)$$

Where, R_n is the net radiation (W/m^2), T_s represents the surface temperature ($^{\circ}C$), α stands for the surface albedo, and NDVI represents the Normalized Difference Vegetation Index. Landuse classification and soil type are considered as important for affecting the value of G and therefore, a landuse map is a valuable source for identification of different surface types.

7. Sensible Heat Flux (H)

Sensible heat flux is defined as the rate of heat loss to the atmosphere because of differences in temperature by the process of convection and conduction. It is calculated by the equation for heat transport. It is calculated from the surface roughness, surface temperature and wind speed.

$$H = (\rho \times c_p \times dT) / r_{ah} \quad (12)$$

Where, ρ represents the density of air (kg/m^3), c_p is the air specific heat ($1004 J/kg/K$), dT (K) represents the difference in temperature ($T_1 - T_2$) between two heights (z_1 and z_2), and r_{ah} shows the aerodynamic resistance to heat transport (s/m).

The aerodynamic resistance to heat transport (r_{ah}) is calculated as,

$$r_{ah} = \frac{\ln\left(\frac{z_2}{z_1}\right)}{u^* \times k} \quad (13)$$

Where, z_1 and z_2 are represented as heights in meters above the zero plane displacement (d) of the vegetation, u^* gives the friction velocity (m/s) that quantifies fluctuations of turbulent velocity in the air, and k represents the von Karman's constant (0.41). The friction velocity (u^*) is calculated by the logarithmic wind law for neutral atmospheric conditions.

$$u^* = \frac{k u_x}{\ln\left(\frac{z_x}{z_{om}}\right)} \quad (14)$$

Where, k stands for the von Karman's constant, u_x shows the wind speed (m/s) at height z_x , and z_{om} represents the roughness length (m) for momentum transport. z_{om} is defined as a measure of the drag and skin friction for the surface air layer.

The wind speed at a particular height above the weather station is considered to remove the effect of the surface roughness. This height is referred as the blending height. The equation 18 is rearranged as,

$$u^* = \frac{ku_{blend}}{\ln\left(\frac{z_{blend}}{z_{om}}\right)} \quad (15)$$

Where; z_{om} represents the particular momentum roughness length for each pixel, u_{blend} is the wind speed at blending height, and z_{blend} represents the blending height. The 200 m is usually considered as the blending height.

The roughness length (z_{om}) for momentum transport is computed empirically from the average height of vegetation around the weather station.

$$z_{om} = 0.12h \quad (16)$$

Where, h shows the vegetation height (m).

The length of momentum roughness (z_{om}) is estimated by two methods of using landuse map and using NDVI and albedo. The landuse maps are used to assign z_{om} values to the non-agriculture and agricultural lands. In case of agricultural land, it is given as,

$$z_{om} = 0.018 \times LAI \quad (17)$$

If landuse maps are not available, then NDVI and albedo data are used to compute z_{om} [4].

$$z_{om} = \exp\left[(a \times NDVI / \alpha) + b\right] \quad (18)$$

Where, a and b are constants of correlation for two or more sample pixels showing a specific vegetation type. The albedo (α) helps in distinguishing between tall and short type of vegetation that may have similar NDVI. The process of estimating iterative process of the sensible heat flux is illustrated in the Figure 1.

The method of SEBAL uses two types of pixels for the fixing of boundary conditions for the energy balance. These two kinds of pixels are “hot” and “cold” pixels from the area of interest. The cold pixel is chosen on the basis of a wet and well-irrigated crop surface covered fully by vegetation. In this pixel, the surface temperature and air temperature near the surface are taken as similar. The hot pixel is selected on the basis of a dry and bare agricultural field that gives almost zero ET.

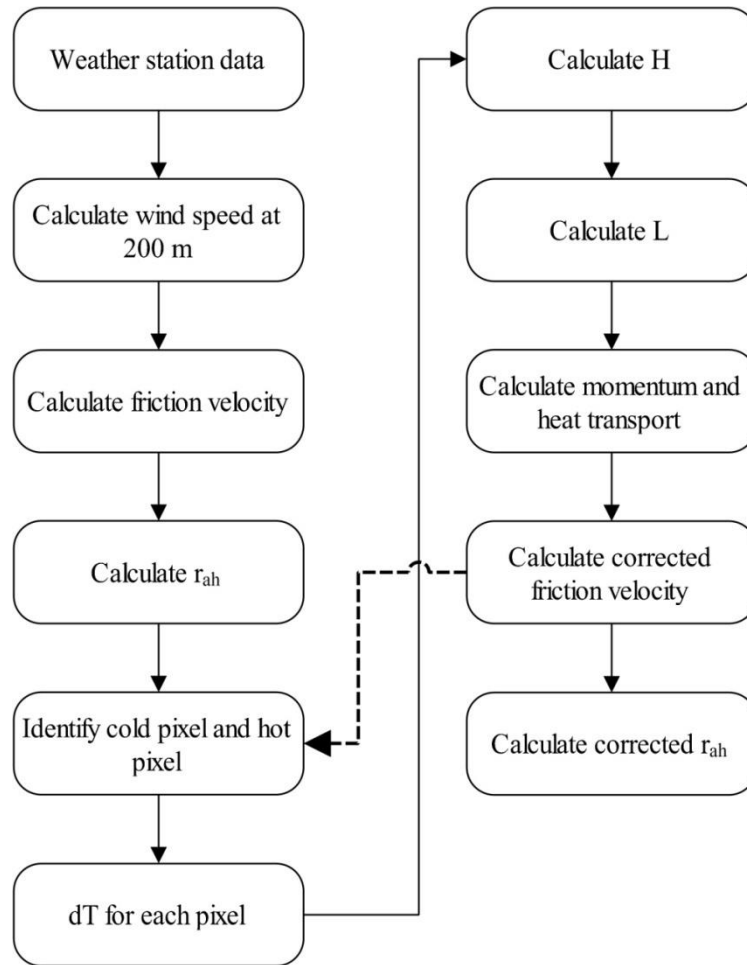


Figure 1 Sensible Heat Flux

The temperature difference or dT of each pixel is required to be defined for computation of sensible heat flux or H . The SEBAL calculates dT by establishing a linear relation between dT and T_s ,

$$dT = b + aT_s \tag{19}$$

Where, a and b are the coefficients of correlation. Two anchor pixels (hot and cold) are used to describe these coefficients, which can estimate the value for H .

At the cold pixel, the sensible heat flux is described as $H_{cold} = R_n - G - \lambda ET_{cold}$. dT_{cold} is computed as,

$$dT_{cold} = H_{cold} \times r_{ah_cold} / (\rho_{cold} \times c_p) \tag{20}$$

At the hot pixel, $H_{hot} = R_n - G - \lambda ET_{hot}$, where ET_{hot} is considered as zero for a hot or dry agricultural area with no green vegetation and dry soil. dT_{hot} is calculated from the Equation 24. Plotting of dT_{cold} against T_{s_cold} and dT_{hot} against T_{s_hot} is given in the Figure 2.

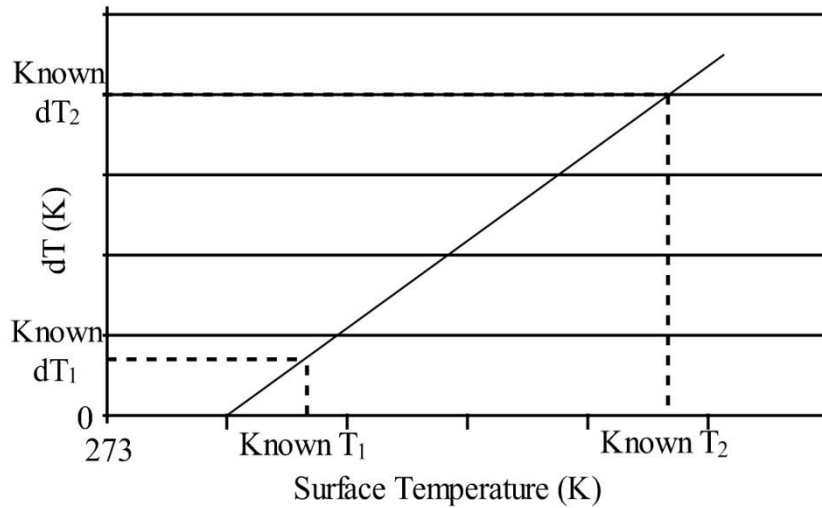


Figure 2 Plotting of dT_{cold} against $T_{s,cold}$ and dT_{hot} against $T_{s,hot}$ (Source: [5])

When the a and b of the sensible heat flux are solved, H is computed for the whole image iteratively until a stable condition is achieved. Finally, the latent heat flux (λET) is calculated for each pixel as a residual of the surface energy balance. Then the instantaneous ET is also computed by the latent heat flux and the latent heat of vaporization.

The Monin-Obukhov length (L) is defined as the condition of stability of the atmosphere achieved in the iterative process. It is considered as a function of the heat and momentum fluxes and is calculated as,

$$L = \frac{\rho c_p u_*^3 T_s}{kgH} \tag{21}$$

Where, ρ represents the air density (kg/m^3), c_p is the air specific heat ($1004 J/kg/K$), u^* is the friction velocity (m/s), T_s represents the surface temperature (K), g stands for the gravitational constant ($9.81 m/s^2$), and H is the sensible heat flux (W/m^2). L values give the atmospheric stability conditions. If $L < 0$, then the atmosphere is considered as unstable, if $L > 0$, then the atmosphere is considered as stable, and if $L = 0$, then the atmosphere is considered as neutral.

On the basis of atmospheric conditions, the stability correction values for momentum and heat transport (ψ_m and ψ_h) are calculated [6-7] as,

When $L < 0$ i.e. unstable condition,

$$\psi_{m(200m)} = 2 \ln \left(\frac{1 + x_{(200m)}}{2} \right) + \ln \left(\frac{1 + x_{(200m)}^2}{2} \right) - 2 ARCTAN(x_{(200m)}) + 0.5\pi \tag{22}$$

$$\psi_{h(2m)} = 2 \ln \left(\frac{1 + x_{(2m)}^2}{2} \right) \tag{23a}$$

$$\psi_{h(0.1m)} = 2 \ln \left(\frac{1 + x_{(0.1m)}^2}{2} \right) \tag{23b}$$

Where,

$$x_{(200m)} = \left(1 - 16 \frac{200}{L}\right)^{0.25} \quad (24a)$$

$$x_{(2m)} = \left(1 - 16 \frac{2}{L}\right)^{0.25} \quad (24b)$$

$$x_{(0.1m)} = \left(1 - 16 \frac{0.1}{L}\right)^{0.25} \quad (24c)$$

When $L > 0$, then stable condition,

$$\psi_{h(200m)} = -5 \left(\frac{2}{L}\right) \quad (25)$$

$$\psi_{h(2m)} = -5 \left(\frac{2}{L}\right) \quad (26a)$$

$$\psi_{h(0.1m)} = -5 \left(\frac{0.1}{L}\right) \quad (26b)$$

When $L = 0$, then neutral conditions where ψ_h and $\psi_m = 0$

A corrected friction velocity (u^*) value is calculated in case of each successive iteration as,

$$u_* = \frac{u_{200} k}{\ln\left(\frac{200}{z_{om}}\right) - \psi_{m(200m)}} \quad (27)$$

Where, u_{200} represents the wind speed at blending height of 200 meters (m/s), k is the von Karman's constant (0.41), z_{om} shows the roughness length for each pixel (m), and $\psi_{m(200m)}$ represents the stability correction for momentum transport at 200 meters.

A value for the aerodynamic resistance to heat transport (r_{ah}) is calculated in the iteration as,

$$r_{ah} = \frac{\ln\left(\frac{z_2}{z_1}\right) - \psi_{h(z_2)} + \psi_{h(z_1)}}{u_* \times k} \quad (28)$$

Where, z_2 is 2 m, z_1 is 0.1 m, and $\psi_{h(z_2)}$ and $\psi_{h(z_1)}$ represent the stability corrections for heat transport at 2 m and 1 m respectively.

Again the equation 23 is repeated for computing new dT values for the hot and cold pixels utilizing the corrected r_{ah} . New values of correlation coefficients a and b are also calculated and dT value for each pixel is recalculated. This process is repeated until the dT_{hot} and r_{ah} become stable.

8. Latent Heat Flux (λET)

The latent heat flux is considered as the latent heat loss rate from the surface of earth because of evapotranspiration. It is calculated as in equation $\lambda ET = R_n - G - H$ where, λET represents the instantaneous value during the satellite overpass (W/m^2).

9. Instantaneous ET (ET_{inst}) and reference ET fraction (ET_rF)

The instantaneous ET is calculated as,

$$ET_{inst} = 3600 \frac{\lambda ET}{\lambda} \quad (29)$$

Where, ET_{inst} represents the instantaneous ET (mm/hr), and λ shows the latent heat of vaporization (J/kg).

The Reference ET Fraction (ET_rF) is considered as the ratio of the instantaneous ET (ET_{inst}) of each pixel to the reference ET (ET_r), which is calculated from the climate data as,

$$ET_r F = \frac{ET_{inst}}{ET_r} \quad (30)$$

Where, ET_r represents the reference ET at the time of the image (mm/hr).

10. Daily actual evapotranspiration (ET_{24})

The daily actual ET (ET_{24}) is calculated from the ET fraction by SEBAL, which is computed as [5],

$$ET_{24} = ET_r F \times ET_{r-24} \quad (31)$$

Where, ET_{r-24} represents the cumulative value of 24-hour ET_r of the image day. It is computed by summing up the hourly ET_r values of the image day.

11. Seasonal actual evapotranspiration ($ET_{seasonal}$)

A seasonal evapotranspiration is obtained from the data of 24-hour evapotranspiration by the process of proportional extrapolation of the ET_{24} to the reference evapotranspiration (ET_r). It is considered that ET of the area of interest changes with respect to the proportional change of ET_r in the weather station. However, ET_r is considered as an index of relative change in weather. The ET:F calculated for the image time is also taken as a constant for the entire period of the image. It is calculated as,

$$ET_{period} = ET_r F_{period} \sum_1^n ET_{r-24} \quad (32)$$

Where, $ET_r F_{period}$ represents ET:F for the period, ET_{r-24} represents the daily ET_r , and n shows the number of days in the period. ET_{period} will be given in mm if ET_{r-24} is given in mm/day.

Markov Chain Model

Future prediction of landuse change is done by using the Markov Chain model. It analyses the landuse classes of different time and date and generates transition matrices and conditional probability images. The matrix indicates the number of pixels that are supposed to change from one class to another over a particular unit of time. The matrix shows the probability of change of a class to every other class. In the Markov Chain model, the change in landuse is the stochastic process and all the different classes are considered to be in a state of the chain. A chain is the stochastic process at time t , X_t , based on the value at $t-1$, X_{t-1} time, and not on the basis of such values as X_{t-2} , X_{t-3} , X_0 , such that the process passed the course in arriving at X_{t-1} [8]. The main equation of Markov model is,

$$P\{X_t = a_j | X_0 = a_0, X_1 = a_1, \dots, X_{t-1} = a_i\} = P\{X_t = a_j | X_{t-1} = a_i\} \quad (33)$$

It is also proper to consider the process of change as the one that is distinctive with time ($t = 0, 1, 2, \dots$).

$P\{X_t = a_j | X_{t-1} = a_i\}$ shows the probability where the process gives transition from state a_i to state a_j within one time period. While, the ℓ steps are needed to implement the transition, the $P\{X_t = a_j | X_{t-1} = a_i\}$ is considered as the transition probability of ℓ step $P_{ij}^{(\ell)}$.

When $P_{ij}^{(\ell)}$ is independent of time and is dependent on states a_i, a_j and ℓ , then the Markov chain is considered as homogeneous. Here,

$$P\{X_t = a_j | X_{t-1} = a_i\} = P_{ij} \quad (34)$$

Where, P_{ij} value is computed from the observed data by the arrangement of the number of times the observed data move from state i to j , n_{ij} , and overall occurrences of the state a_i , n_i is summed up.

$$P_{ij} = n_{ij} / n_i \quad (35)$$

With the process of time in the Markov chain model, the probability at which it retains in state j becomes independent of the initial state of the chain after several steps. When there is a occurrence of such condition, a steady state is believed to have reached by the chain. Then P_j , which is considered as the limit probability, is used to decide the value of $P_{ij}^{(\ell)}$,

$$\lim_n P_{ij}^{(n)} = P_j \quad (36)$$

Where,

$$P_j = P_i P_{ij}^{(n)} \quad j=1, 2, \dots, m \text{ (state)}$$

$$P_i = 1 \quad P_j > 0$$

References:

1. Allen, R.G. Using the FAO-56 dual crop coefficient method over an irrigated region as part of an evapotranspiration intercomparison study. *J. Hydrol.* **2000**, *229*, 27–41.
2. Bastiaanssen, W.G.M. Regionalization of surface flux densities and moisture indicators in composite terrain. In a Remote Sensing Approach under Clear Skies in Mediterranean Climates. 1995. Available online: <http://library.wur.nl/WebQuery/wda/918192> (accessed on 10 May 2012)
3. Goetz, S. J. Multi-sensor analysis of NDVI, surface temperature and biophysical variables at a mixed grassland site. *Int. J. Remote Sens.* **1997**, *18*, 71–94.
4. Bastiaanssen, W. G. M. SEBAL-based sensible and latent heat fluxes in the irrigated Gediz Basin, Turkey. *J. Hydrol.* **2000**, *229*, 87–100.
5. Allen, R.; Tasumi, M.; Trezza, R.; Waters, R.; Bastiaanssen, W. Sebal (surface energy balance algorithms for land). In Advance Training and Users Manual—Idaho Implementation, Version; 2002; Volume 1, p. 97. Available online: <http://https://www.researchgate.net/file.PostFileLoader.html?id=5635f25060614b180d8b4567&assetKey=AS%3A290936253894656%401446376016229> (accessed on 8 May 2012).

6. Paulson, C. A. The mathematical representation of wind speed and temperature profiles in the unstable atmospheric surface layer. *J. Appl. Meteorol.* **1970**, *9*, 857–861.
7. Webb, E. K. Profile relationships: The log-linear range, and extension to strong stability. *Q. J. R. Meteorol. Soc.* **1970**, *96*, 67–90.
8. Weng, Q. Land use change analysis in the Zhujiang Delta of China using satellite remote sensing, GIS and stochastic modelling. *J. Environ. Manag.* **2002**, *64*, 273–284.